

<https://doi.org/10.15407/knit2023.03.016>
UDC 629.7.05; 681.5.015

N. N. SALNIKOV, Principal Researcher, Doctor of Physical and Mathematical Sciences
ORCID <https://orcid.org/0000-0001-9810-0963>
E-mail: salnikov.nikolai@gmail.com.

S. V. MELNYCHUK, Senior Researcher, Candidate of Technical Sciences
ORCID <https://orcid.org/0000-0002-6027-7613>
E-mail: sergvik@ukr.net.

V. F. GUBAREV, Head of Department, Corresponding Member of the NAS of Ukraine,
Professor, Doctor of Technical Sciences
ORCID <https://orcid.org/0000-0001-6284-1866>
E-mail: v.f.gubarev@gmail.com.

L. V. MAKSYMUK, Researcher, Candidate of Technical Sciences
ORCID <https://orcid.org/0000-0002-2561-109X>
E-mail: hatahatky@gmail.com.

V. M. SHEVCHENKO, Senior Researcher, Candidate of Physical and Mathematical Sciences
ORCID <https://orcid.org/0000-0002-1304-9124>
E-mail: vovan_16@ukr.net.

Space Research Institute of the National Academy of Sciences of Ukraine and the State Space Agency of Ukraine
40, build. 4/1, Akademika Glushkova Ave., Kyiv, 03187 Ukraine

RELATIVE MOTION PARAMETERS ESTIMATION OF A NON-COOPERATIVE SPACECRAFT FROM VISUAL INFORMATION

In this work, we consider the problem of determining parameters of the relative motion of a non-cooperative spacecraft (NSC), which is in free uncontrolled motion, based on the results of measuring the distance to this vehicle and its attitude quaternion. The measurements are assumed to be made by some computer vision system (CVS). A specific type of CVS is not considered. It is supposed the CVS measures the distance and attitude of the so-called graphical reference frame rigidly fixed on the NSC. The parameters of relative motion include the distance vector to the center of mass (c.m.) of the NSC, the attitude quaternion of the principal inertia axes of the NSC relative to the CVS reference frame, the attitude quaternion of the graphical reference frame relative to the NSC principal reference frame, the ratio of the inertia moments, the position vector of the c.m. in the graphical reference frame.

The problem is solved using a dynamic filter based on the ellipsoidal estimation method. The method implies knowledge of the maximum values of the measurement noise only, the stochastic noise characteristics are not assumed to be known and therefore are not used. The properties of the proposed algorithm have been demonstrated using numerical simulations. The results obtained are supposed to be used in the development, creation, and testing of a navigation system for the rendezvous and docking of a service spacecraft, developed by a group of enterprises in the space industry of Ukraine under the leadership of the Limited Liability Company “Kurs–Orbital”.

Keywords: *relative motion parameters, spacecraft, estimation, video image.*

Цитування: Salnikov N. N., Melnychuk S. V., Gubarev V. F., Maksymyuk L. V., Shevchenko V. M. Relative motion parameters estimation of a non-cooperative spacecraft from visual information. *Space Science and Technology*. 2023. **29**, № 3 (142). P. 16–33. <https://doi.org/10.15407/knit2023.03.016>

© Publisher ПН «Академперіодика» of the NAS of Ukraine, 2023. This is an open access article under the CC BY-NC-ND license (<https://creativecommons.org/licenses/by-nc-nd/4.0/>)

INTRODUCTION

In near-Earth space, the number of space objects related to space debris is growing. Some of these objects are non-operational spacecrafts, which, with minor repairs or after refueling, can continue their work. Therefore, there is a need to create the so-called service spacecraft (SSC) capable of docking with a non-cooperative spacecrafts (NSC) or some space objects and performing maintenance, change of the orbit, or removal of the object from the orbit. Development of such spacecrafts has been carried out for the past 20 years in many space technology centers around the world. The current state of this problem can be found in reviews [35, 38, 47].

It is known [8, 10, 19, 20] that the success in the implementation of the docking significantly depends on the accuracy of determining the relative navigation of NSC and SSC. It is assumed that the NSC is not equipped with navigation and attitude control systems, or they do not work for some reason. In this case, radar and optical systems settled at SSC are used to determine the relative position and orientation of the NSC. The latter include laser [1, 2, 5, 37, 39] and purely optical systems [11, 16–18, 21–23, 25, 31, 34, 36, 40, 43, 49–51, 54, 57, 58], which use cameras operating in the optical range. Optical systems are used at the final stage of docking at close distances (no more than 100 m) because they are able to provide a more accurate measurement of parameters of the relative position and attitude of the NSC. Using the appropriate software, these devices allow measuring the distance to and orientation of a certain coordinate system that is rigidly fixed to the NSC relative to the device reference frame. It can be some assembly reference frame in which the position of every NSC construction element is given. Anyway, the measured information is not enough for trajectory planning and docking with the NSC. This is due, among other things, to the fact that the NSC, as established by observations [26, 27, 46], eventually begins to rotate around the center of mass. This happens due to the action of the gravitational moment, cosmic radiation, and the flow of solar wind particles [32]. For docking, it is also necessary to know the time evolution of the relative position and speed of the docking surface position. These quantities can be

obtained only by knowing all the parameters of the angular and orbital motion of the NSC. At present, there are a large number of works devoted to solving the problem of estimating these parameters [1–5, 11, 25, 37, 39, 49, 53, 58]. These works used various versions of the Kalman filter [7, 13, 24] for estimation.

The Kalman filter is known to be based on the assumption that the uncertainties are normally distributed random variables. The distribution parameters are assumed to be known. But determining these parameters in practice is a separate, rather laborious task. For half a century, a different approach has been developed [9, 12, 14, 28, 29, 42, 48] to the problem of estimating unknown quantities, in particular, estimating the state vector of dynamic systems, which is based on the use of minimal information about uncertain quantities. According to this approach, only sets of possible values of these quantities are assumed to be known. As a result, the estimation process is reduced to procedures for calculating the evolution of the sets and performing set-theoretic operations on them, i.e., to the construction of refined sets or, as they are usually called, information sets that are guaranteed to contain the estimated values. In accordance with this, such an approach is called guaranteed or set-theoretic. In most cases, the construction of the information sets is associated with serious computational difficulties, which is an obstacle to their implementation in on-board computer systems. The ellipsoidal estimation method [9, 12, 14, 29, 42, 48] seems to be quite effective concerning its functionality and minimization of computational costs. Following this method, information sets are approximated by multidimensional ellipsoids. The ellipsoidal estimation method is sensitive to the violation of a priori assumptions about the value of uncertain quantities. To withdraw this property, i.e., to ensure the robustness property, several modifications of this method have been proposed [44, 45, 55, 56].

This work aims to develop an algorithm for estimating parameters of the angular motion of an NSC (attitude quaternion, angular velocity vector, ratio of inertia moments, position of the principal axes of inertia, and position of the center of mass) and distance to the NSC based on the modification of ellipsoidal estimation method [44, 45]. Information on the rela-

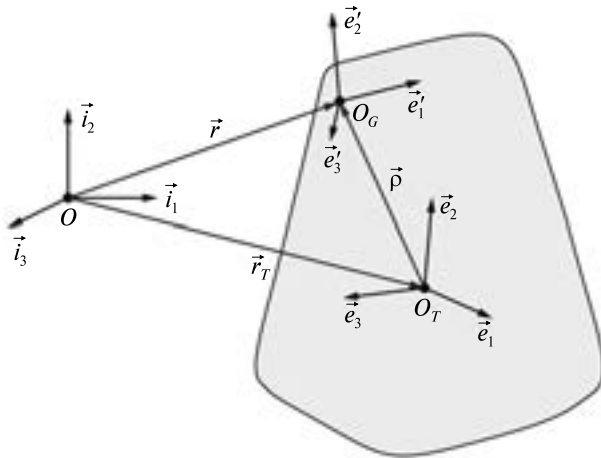


Figure 1. Reference frames

tive position of the NSC is provided by CVS. The algorithm is planned to be used for full-scale bench tests. Due to this reason, it is assumed that the CVS camera position is fixed in some inertial reference frame. Any of the relative navigation devices mentioned above can be considered as such a CVS device. The authors of this work focused on the use of the CVS, the principle of operation and algorithms of which are described in [22, 43]. The proposed algorithms use the multiplicative form of quaternion increments [15, 30, 33], which not only eliminates, in fact, the heuristic procedure of quaternion normalization, which is required when using the additive form of increment but also leads to simpler equations describing the dynamics of quaternion increments. This work is a development of [54] and is very close to [3] in the problem statement.

1. PROBLEM STATEMENT OF ESTIMATING THE NSC MOTION PARAMETERS

1.1. Coordinate systems and their relative positions. The NSC motion is considered in 3-dimensional real Euclidian space R^3 . Let us denote the inertial reference frame in this space with origin at point O , and orthonormal basis vectors $i_j, j=1:3$, by the symbol $Oi_1i_2i_3$, or simply OI . The body reference frame $O_Ge'_1e'_2e'_3$, which will be further referred to as the graphical one, is fixed to the NSC. It can be an assembly reference frame in which positions of all the NSC construction elements are given (see Fig. 1).

The CVS measures the distance vector between the points O and O_G , and the attitude quaternion

$$\eta = \eta_0 + \sum_{j=1}^3 \eta_j i_j = \eta_0 + \eta_v \quad (1)$$

of graphical reference frame $O_Ge'_1e'_2e'_3$ relative to the frame $Oi_1i_2i_3$. The scalar part of a quaternion is determined by a real number η_0 , the vector part by a vector

$$\eta_v = \sum_{j=1}^3 \eta_j i_j$$

[6, 19]. The set of numbers $\eta_j, j=0:3$, are called quaternion coordinates in the basis $Oi_1i_2i_3$. A quaternion η is called normalized if its norm

$$\|\eta\| = \eta_0^2 + \eta_1^2 + \eta_2^2 + \eta_3^2 = 1. \quad (2)$$

A normalized quaternion defines a rotation of the three-dimensional Euclidean space as a whole about an axis defined by a vector e by an angle ϕ , and $\eta_0 = \cos(\phi/2)$ and $\eta_v = \sin(\phi/2)e/\|e\|$. When performing two successive rotations defined by the quaternions q and μ , the resulting rotation will be determined by the quaternion

$$\eta = \mu \circ q, \quad (3)$$

where the quaternion multiplication operation $\mu \circ q$ is defined as follows

$$\mu \circ q = \mu_0 q_0 - (\mu_v \cdot q_v) + \mu_0 q_v + q_0 \mu_v + \mu_v \times q_v. \quad (4)$$

Here, $(\mu_v \cdot q_v)$ is the scalar product of vectors μ_v and q_v , $\mu_v \times q_v$ is the vector product. Quaternion coordinates depend on the choice of reference frame. Therefore, to calculate the quaternion coordinates of η using (4), the quaternion coordinates q and μ must be expressed in one coordinate system.

The body reference frame $O_T e_1 e_2 e_3 = O_T E$ is also fixed at the NSC. Its center is located at the center of mass (c.m.) of the NSC, and the unit vectors $e_j, j=1:3$, are oriented along the principal axes of the inertia tensor. This frame will be called as principal reference frame. The position of $O_T E$ is unknown and is characterized by an unknown normalized quaternion

$$q = q_0 + \sum_{j=1}^3 q_j i_j = q_0 + q_v$$

relative to the inertial reference frame $Oi_1i_2i_3$. This means [6] that the basis vectors $e_i, i=1:3$, of the reference frame $O_T E$ are obtained by rotating the

basis vectors i_j , $j=1:3$, in accordance with the following expression

$$e_j = q \circ i_j \circ \bar{q}, \quad j=1:3, \quad (5)$$

where the vector i_j should be considered as a quaternion with a zero scalar part, $\bar{q} = q_0 - q_v$ is a quaternion conjugated to q , $\bar{q} \circ q = q \circ \bar{q} = 1$.

The position of the vectors e'_i , $i=1:3$, with respect to the basis vectors e_i , $i=1:3$, will be characterized by the quaternion

$$\mu = \mu_0 + \sum_{j=1}^3 \mu_j e_j = \mu_0 + \mu_v, \quad (6)$$

which is also considered to be unknown but constant

$$\dot{\mu}_j = 0, \quad j=0:3. \quad (7)$$

The angular position of the graphical reference frame $O'e'_1e'_2e'_3$ relative to the inertial one $O_i i_2 i_3$ is determined by the quaternion $\eta = \mu \circ q$, i.e. by the expression (3). To obtain the quaternion expression η in the basis i_j , $j=1:3$, we substitute (5) into (6). As a result, we get

$$\begin{aligned} \eta &= \mu \circ q = \left(\mu_0 + \sum_{j=1}^3 \mu_j e_j \right) \circ q = \\ &= q \circ \left(\mu_0 + \sum_{j=1}^3 \mu_j i_j \right) \circ \bar{q} \circ q = q \circ \mu^*, \end{aligned} \quad (8)$$

where the quaternion

$$\mu^* = \left(\mu_0 + \sum_{j=1}^3 \mu_j i_j \right).$$

Both quaternion q and μ^* on the right side of (8) are expressed in the basis i_j , $j=1:3$. We will use further the expression (8) for the quaternion η but will not write an asterisk for the quaternion μ^* .

A quaternion η is characterized by a set of its coordinates, which can be formed in a vector $\eta = (\eta_0, \eta_1, \eta_2, \eta_3)^T \in R^4$. We will denote the quaternion and the vector of its coordinates by the same symbol, but remember that quaternion coordinates depend on the used reference frame. Using the definition of quaternion multiplication (4) for the vector representation of quaternions, it is easy to obtain the following vector-matrix relations

$$\eta = q \circ \mu = Q(q)\mu = \bar{Q}(\mu)q, \quad (9)$$

where 4×4 -matrices

$$\begin{aligned} Q(q) &= \begin{pmatrix} q_0 & -q_v^T \\ q_v & (q_0 I_3 + [q_v \times]) \end{pmatrix}, \\ \bar{Q}(\mu) &= \begin{pmatrix} \mu_0 & -\mu_v^T \\ \mu_v & (\mu_0 I_3 - [\mu_v \times]) \end{pmatrix}. \end{aligned}$$

In these expressions, I_3 is the identity 3×3 -matrix,

$$[q_v \times] = \begin{pmatrix} 0 & -q_3 & q_2 \\ q_3 & 0 & -q_1 \\ -q_2 & q_1 & 0 \end{pmatrix}$$

is the cross product matrix, $[q_v \times] \mu_v = q_v \times \mu_v$.

For the vector representation of the quaternion η , which determines the rotation around the unit vector $e = \eta_v / \|\eta_v\|$ by an angle ϕ , the following representation is true

$$\eta = (\eta_0, \eta_1, \eta_2, \eta_3)^T = \begin{pmatrix} \cos(\phi/2) \\ \sin(\phi/2)e \end{pmatrix}, \quad (10)$$

where vector e contains coordinates of this vector in some reference frame.

1.2. Basic equations of the NSC motion. It is assumed that the NSC is in a state of rotation, described by the following equation

$$J \frac{d\omega}{dt} + [\omega \times] J \omega = M. \quad (11)$$

Here, the angular velocity vector $\omega = (\omega_1, \omega_2, \omega_3)^T$ is represented by its coordinates in the principal reference frame $Oe_1e_2e_3$ (OE), the axes of which are directed along the principal axes of inertia of the NSC. Therefore, the inertia tensor matrix in equation (11) is diagonal

$$J = \text{diag}\{J_1, J_2, J_3\}$$

The principal moments of inertia J_i , $i=1:3$, are considered to be unknown. The moment M in equation (11) includes the gravitational moment, aerodynamic and other moments due to the action of the environment on the NSC [32]. We assume that the influence of these moments on the angular position of the NSC during its revolution around the Earth can be neglected, i.e., in equation (11), we set

$$M = 0. \quad (12)$$

It is easy to notice that in the absence of the moment of external forces, the solutions of equation

(11) depend only on the ratio of the inertia moments. Let us introduce the following notation

$$p_1 = J_1 J_3^{-1}, p_2 = J_2 J_3^{-1}. \quad (13)$$

Then equations (11) can be written in the following form

$$\begin{cases} \dot{\omega}_1 = p_1^{-1}(p_2 - 1)\omega_2\omega_3; \\ \dot{\omega}_2 = p_2^{-1}(1 - p_1)\omega_1\omega_3; \\ \dot{\omega}_3 = (p_1 - p_2)\omega_1\omega_2. \end{cases} \quad (14)$$

Obviously, the solutions of this equation and equation (11) under condition (12) and with the same initial conditions completely coincide when (13) is held. We assume the inertia moments are constant over the considered time interval. Therefore, the vector $p = (p_1, p_2)^T$ satisfies the following equation

$$\dot{p} = 0. \quad (15)$$

The change in time of the quaternion $q = q(t)$ is related to the angular velocity

$$\omega = \sum_{j=1}^3 \omega_j e_j$$

of the NSC rotation by the following equation [6, P. 26]

$$\dot{q} = \frac{1}{2} q \circ \omega^*, \quad (16)$$

where coordinates of the vector

$$\omega^* = \sum_{j=1}^3 \omega_j i_j$$

are the coordinates of the NSC angular velocity in the NSC principal reference frame OE . The initial conditions for equations (11) and (16) are unknown.

1.3. Measurement Equations. The position of the origin O_G of the graphical reference frame $O_G E'$ is determined by the vector r in the inertial reference frame OI and measured by the CVS. The measured vector

$$r = r_T + \rho, \quad (17)$$

where r_T is the position vector of the NSC c.m. in the inertial reference frame OI . It is assumed to be constant but unknown

$$\dot{r}_T = 0. \quad (18)$$

The vector $\rho = O_G - O_T$ giving the position of the point O_G in the principal reference frame $O_T E$, is

also unknown and is constant in this frame, i.e.

$$\rho = \sum_{j=1}^3 \rho_j e_j, \quad (19)$$

where

$$\dot{\rho}_j = 0, \quad j = 1:3. \quad (20)$$

Let us express the coordinates of the vector ρ in the inertial reference frame. Substituting (5) into (19) we get

$$\begin{aligned} \rho &= \sum_{j=1}^3 \rho_{I,j} i_j = \sum_{j=1}^3 \rho_j e_j = \sum_{j=1}^3 \rho_j (q \circ i_j \circ \bar{q}) = \\ &= q \circ \left(\sum_{j=1}^3 \rho_j i_j \right) \circ \bar{q}. \end{aligned}$$

Whence, using representation (9), we obtain

$$\rho_I = R(q)\rho, \quad (21)$$

where vectors $\rho_I = (\rho_{I,1}, \rho_{I,2}, \rho_{I,3})^T$, $\rho = (\rho_1, \rho_2, \rho_3)^T$ and 3×3 -matrix

$$R(q) = (q_0^2 - q_v^T q_v) I_3 + 2q_0 [q_v \times] + 2q_v q_v^T. \quad (22)$$

Expression (21) is obtained using the vector-matrix representation (9) of the quaternion multiplication operation

$$Q(q) \bar{Q}(\bar{q}) = \begin{pmatrix} \|q\| & \Theta_{1 \times 3} \\ \Theta_{3 \times 1} & R(q) \end{pmatrix}.$$

Here $\Theta_{m \times n}$ is the null $m \times n$ -matrix. Then from (17) and (21) we obtain the following equality for the vector coordinates

$$r = r_T + R(q)\rho.$$

We assume the measurements of the quaternion η and vector r are made at discrete time $t_k = t_0 + \Delta \cdot k$, $k = 0, 1, 2, \dots$, with additive bounded errors ξ_k^r and ξ_k^η , i.e., the following measurement vectors are obtained

$$\check{r}_k = r(t_k) + \xi_k^r = r_k + \xi_k^r = r_{T,k} + R(q_k)\rho_k + \xi_k^r, \quad (23)$$

$$\check{\eta}_k = \eta(t_k) + \xi_k^\eta = \eta_k + \xi_k^\eta = q_k \circ \mu_k + \xi_k^\eta. \quad (24)$$

The measurement errors satisfy the following inequalities

$$\|\xi_k^r\|_\infty \leq c_r, \quad \|\xi_k^\eta\|_\infty \leq c_\eta,$$

where $c_r > 0$ and $c_\eta > 0$ are the maximum values of errors assumed to be known. From here, (23) and (24), it follows that the unknown parameters of the

NSC motion satisfy the following inequalities

$$\begin{aligned} \|\tilde{r}_k - r_{T,k} - R(q_k)\rho_k\|_\infty &\leq c_r, \\ \|\tilde{\eta}_k - q_k \circ \mu_k\|_\infty &\leq c_\eta \quad \forall k \geq 0. \end{aligned} \quad (25)$$

1.4. Estimation problem statement. Differential equations (7), (14)–(16), (18), (20) can be considered as equations of a nonlinear dynamical system in continuous time, the state vector of which has the form

$$x = (\omega^T, q^T, p^T, r_T^T, \rho^T, \mu^T)^T \in R^{19}. \quad (26)$$

The initial conditions for these equations are unknown. At discrete times t_k , some components of this vector $x_k = x(t_k) = (\omega_k^T, q_k^T, p_k^T, r_{T,k}^T, \rho_k^T, \mu_k^T)^T$ must satisfy measurement inequalities (25). In addition, the normalization conditions (2) must be satisfied for the components q and μ of the vector x .

Let \hat{x}_{k-1} be some estimate of the state vector x_{k-1} obtained at a discrete time moment $(k-1)$. Using differential equations (7), (14)–(16), (18), (20), we can calculate the estimate $\hat{x}_{k|k-1}$ for the time moment k . If this estimate satisfies inequalities (25), then, obviously, it is not necessary to refine it and we can set $\hat{x}_k = \hat{x}_{k|k-1}$. If the estimate $\hat{x}_{k|k-1}$ does not satisfy at least one of the inequalities (25), then its refinement is required.

The problem is to find such a method for refining estimates \hat{x}_k , in which inequalities (25) will be satisfied, starting from some finite time moment K . Ideally, this method should satisfy the limit

$$\lim_{k \rightarrow \infty} \|\hat{x}_k - x_k\| = 0.$$

However, its existence is associated with the implementation of certain properties of measurement noise, which are difficult to verify and ensure in practice.

2. METHOD OF ESTIMATING THE NSC RELATIVE POSE PARAMETERS

In this paper, we use a set-theoretic or guaranteed approach to state estimation of dynamical systems, which needs to use minimal a priori information about uncertain values. With respect to these quantities, only the sets of their possible values are assumed to be known. In this case, the estimation procedure is reduced to performing operations on sets in order to construct so-called information sets that are guar-

anteed to contain the estimated values. In this work, the modification [44, 45] of ellipsoidal estimation algorithms [9, 12, 14, 29, 42, 48, 55, 56] was used. The main advantages of the modification are the minimum of a priori information about uncertain quantities, the high convergence rate, its applicability to nonlinear systems, and resistance to possible violations of a priori hypotheses about the values of uncertain quantities.

2.1. Guaranteed approach to estimating the state vector of dynamical systems. Let us briefly describe the essence of the guaranteed approach to state estimation of dynamical systems. Equations (7), (14)–(16), (18), (20), using definition (26) of the state vector, can be written as

$$\dot{x} = f(x(t), u(t), \zeta(t)), \quad t \geq t_0, \quad (27)$$

where $x(t) \in R^n$ is the state vector at continuous time moment t , $u(t)$ is the vector of measured input variables, $\zeta(t)$ is the vector of uncontrolled perturbations. We will assume that the functions $f(\cdot)$, $u(\cdot)$, and $\zeta(\cdot)$ are such that the standard conditions [41] for the existence and uniqueness of a solution to Eq. (27) are satisfied. We assume that the vector

$$\zeta(t) \in Z \quad \forall t, \quad (28)$$

where Z is some bounded closed set.

Inequalities (25) associated with measurements can be written in the following form

$$|g_j(x_k) - y_{j,k}| \leq c_j, \quad j=1:N, \quad \forall k \geq 0, \quad (29)$$

where $g_j(x): R^n \rightarrow R$, $j=1:N$, are continuously differentiable functions of the state vector x , y_{jk} is output measurement, $N=7$. These inequalities are considered for discrete measurement moments t_k . In addition, the normalization condition (2) for the quaternions included in the state vector must be satisfied.

We now describe the procedure for refining information about the state vector according to the guaranteed or set-theoretic approach to estimation. Assume that at the moment of time t_k it is known that the state vector

$$x_k = x(t_k) \in X_k, \quad (30)$$

where the set X_k is given. Considering equation (27) on the time interval $[t_k, t_{k+1}]$ for all possible x_k satisfying (30) and for all possible realizations of

perturbations $\zeta(\cdot)$ satisfying condition (28) on this interval, we can obtain the set

$$X_{k+1|k} = \{x = x(t_{k+1}, x_k, u(\cdot), \xi(\cdot)), \\ \forall x_k \in X_k \forall \zeta(\tau) \in Z \forall \tau \in [t_k, t_{k+1}]\}$$

of possible values of the vector $x_{k+1} = x(t_{k+1})$ at a discrete time $k+1$. The construction of this set can be carried out, for example, by integrating the equation (27) on the interval $[t_k, t_{k+1}]$ under various initial conditions satisfying (30) and for all possible realizations of perturbations $\zeta(\tau) \in Z \forall \tau \in [t_k, t_{k+1}]$. Obviously, this is a very time-consuming process that requires a lot of calculations.

On the other hand, at the moment of time t_{k+1} the state vector x_{k+1} satisfies inequalities (29), that can be written as

$$x_{k+1} \in \bar{X}_{k+1} = \{x : |g_j(x) - y_{j,k+1}| \leq c_j, \quad j = \overline{1, N}\}. \quad (31)$$

The set \bar{X}_{k+1} contains state vectors that are compatible with the measurements under given a priori constraints on the measurement noise values. As a result, we can conclude that

$$x_{k+1} \in X_{k+1} = \bar{X}_{k+1} \cap X_{k+1|k}.$$

Despite the obvious simplicity and logical rigor of the presented approach for refining the set of possible values of the state vector, its practical implementation in the general case encounters insurmountable computational difficulties associated with the construction and description of the sets $X_{k+1|k}$, \bar{X}_{k+1} , X_{k+1} , as well as the implementation of set-theoretic operations, in the considered case, the set intersection operation.

One of the approaches aimed at reducing the computational complexity of solving estimation problems is to use the ellipsoid method [9, 12, 14, 29, 42, 48, 55, 56]. In accordance with this method, the set X_k is considered to be an ellipsoid

$$X_k = E_k = E(\hat{x}_k, H_k) = \{x : (x - \hat{x}_k)^T H_k^{-1} (x - \hat{x}_k) \leq 1\},$$

given by a center vector \hat{x}_k and a positive-definite symmetric matrix $H_k = H_k^T > 0$. The notation $E(\hat{x}_k, H_k)$ will be used frequently in what follows. The ellipsoid $E_k = X_k$ in (30) is commonly referred to as the ellipsoidal estimate of vector x_k . The center of the ellipsoid, the vector \hat{x}_k , is taken as a point estimate. Ellipsoidal approximations for the sets

$X_{k+1|k}$ and X_{k+1} are constructed in the form of containing them ellipsoids $E_{k+1|k} = E(\hat{x}_{k+1|k}, H_{k+1|k})$ and $E_{k+1} = E(\hat{x}_{k+1}, H_{k+1})$, correspondingly. The solution of the estimation problem is reduced to constructing a sequence $\{E_k\}_{k=0}^\infty$ of ellipsoidal estimates E_k for the vector x_k in accordance with the following recurrent procedure

$$x_{k+1} \in E_{k+1} = [\bar{X}_{k+1} \cap [X_{k+1|k}]_E]_E = [\bar{X}_{k+1} \cap E_{k+1|k}]_E. \quad (32)$$

Here $[X]_E$ denotes the operation of covering a bounded set $X \subset R^n$ by a minimal in a certain sense ellipsoid E , i.e. $X \subset E$. Its volume, diameter, or another function characterizing the size of the ellipsoid is usually considered as a criterion for choosing such an ellipsoid. The described method for constructing ellipsoidal estimates is called ellipsoidal estimation method. For linear systems, many operations $[X]_E$ have been developed that are optimal and suboptimal in some sense. In the case of nonlinear systems, the operation $[X]_E$ can generally be implemented only numerically and requires a large amount of computation.

2.2. Application of the modified ellipsoidal estimation method. A heuristic approach proposed in [44, 45], makes it possible to reduce the amount of calculations when constructing a sequence of ellipsoidal estimates, significantly increase the rate of convergence, and also make the estimation algorithm robust with respect to violations of a priori assumptions on the properties of uncertain values. A similar approach was previously proposed and studied in [55, 56]. According to approach [45], the ellipsoid $E_{k+1|k} = E(\hat{x}_{k+1|k}, H_{k+1|k})$ is constructed using linear part of the expansion of the function $f(\cdot)$ in the vicinity of the point \hat{x}_k , as in the extended Kalman filter. Its center $\hat{x}_{k+1|k}$ is found by numerically integrating the following equation

$$d\tilde{x} / dt = f(\tilde{x}(t), u(t), \hat{\zeta}(t)), \quad \tilde{x}(t_k) = \hat{x}_k, \quad t \in [t_k, t_{k+1}],$$

assuming $\hat{x}_{k+1|k} = \tilde{x}(t_{k+1})$. Here $\hat{\zeta}(t)$ is the estimate of the unknown vector $\zeta(t)$, chosen on the basis of some considerations. Usually it is assumed that $\hat{\zeta}(t) = 0$.

For the quantity

$$\Delta x(t) = x(t) - \tilde{x}(t),$$

using the Taylor series expansion, the following equation can be obtained

$$\begin{aligned}
 \frac{d\Delta x}{dt} &= f(x(t), u(t), \zeta(t)) - f(\tilde{x}(t), u(t), \hat{\zeta}(t)) = \\
 &= f(\tilde{x}(t) + \Delta x, u(t), \hat{\zeta}(t) + \Delta \zeta(t)) - f(\tilde{x}(t), u(t), \hat{\zeta}(t)) = \\
 &= \partial_x f(\tilde{x}(t), u(t), \hat{\zeta}(t)) \Delta x + \partial_\zeta f(\tilde{x}(t), u(t), \hat{\zeta}(t)) \Delta \zeta(t) + \\
 &\quad + o_x(\|\Delta x\|) + o_\zeta(\|\Delta \zeta\|), \quad t \in [t_k, t_{k+1}]. \quad (33)
 \end{aligned}$$

Here, the vector functions $o_x(\|\Delta x\|)$ and $o_\zeta(\|\Delta \zeta\|)$ denote expansion terms of the second order of smallness with respect to Δx and $\Delta \zeta$. These terms can be discarded and we obtain linear equation from (33). This equation allows in general to calculate the matrix $H_{k+1|k}$ of the ellipsoid $E_{k+1|k}$, but again the computational costs may be unreasonably high. Therefore, calculation of the matrix $H_{k+1|k}$ is proposed [45] to perform with the use of the following stationary linear equation

$$\frac{d\Delta x}{dt} = A_k \Delta x, \quad t \in [t_k, t_{k+1}], \quad (34)$$

where $n \times n$ -matrix

$$A_k = \partial_x f(\hat{x}_{k+1/2}, u_{k+1/2}, \hat{\zeta}_{k+1/2}).$$

Here

$$\begin{aligned}
 \hat{x}_{k+1/2} &= 0.5 \cdot (\hat{x}_{k+1|k} + \hat{x}_k), \\
 u_{k+1/2} &= \frac{1}{\Delta} \int_{t_k}^{t_{k+1}} u(\tau) d\tau, \\
 \hat{\zeta}_{k+1/2} &= \frac{1}{\Delta} \int_{t_k}^{t_{k+1}} \hat{\zeta}(\tau) d\tau.
 \end{aligned}$$

If $\Delta x_k \in E(0, H_k)$, then by virtue of equation (34) it can be obtained [55] that

$$\Delta x(t_{k+1}) \in E(0, H_{k+1|k}),$$

where

$$H_{k+1|k} = A_k H_k A_k^T. \quad (35)$$

Here $n \times n$ -matrix $A_k = \exp(A_k \cdot \Delta)$. We finally take

$$\begin{aligned}
 E_{k+1|k} &= E(\hat{x}_{k+1|k}, H_{k+1|k}) = \\
 &= \{x : (x - \hat{x}_{k+1|k})^T H_{k+1|k}^{-1} (x - \hat{x}_{k+1|k}) \leq 1\}.
 \end{aligned}$$

In this case due to the used approximation $E_{k+1|k} \neq X_{k+1|k}$ in general, i.e., some ends of the trajectories of system (27) that have left the set $X_k = E_k$ will not belong to $E_{k+1|k}$.

The following estimate of the set \bar{X}_{k+1} is also considered

$$\hat{X}_{k+1} = \bigcap_{j=1}^N \Pi_{j,k+1},$$

where sets

$$\begin{aligned}
 \Pi_{j,k+1} &= \{x : |\nabla g_j^T(\hat{x}_{k+1|k})(x - \hat{x}_{k+1|k}) + \\
 &\quad + g_j(\hat{x}_{k+1|k}) - y_{j,k+1}| \leq c_j\}, \quad j = 1:N \quad (36)
 \end{aligned}$$

are obtained from (31) by replacing the function $g_j(x)$ with its linear approximation in the vicinity of the point $\hat{x}_{k+1|k}$. In general $\hat{X}_{k+1} \neq \bar{X}_{k+1}$. Due to this and the fact that $E_{k+1|k} \neq X_{k+1|k}$, it may turn out that $E_{k+1|k} \cap \hat{X}_{k+1} = \emptyset$. In this case it is impossible to implement an analog of the scheme (32) for constructing an ellipsoid E_{k+1} in the form $E_{k+1} = [E_{k+1|k} \cap \hat{X}_{k+1}]_E$. Therefore, in the case $E_{k+1|k} \cap \hat{X}_{k+1} = \emptyset$ it is proposed to take a widened ellipsoid instead of an ellipsoid $E_{k+1|k}$, that is

$$\tilde{E}_{k+1|k} = \{x : (x - \hat{x}_{k+1|k})^T \tilde{H}_{k+1|k}^{-1} (x - \hat{x}_{k+1|k}) \leq 1\}, \quad (37)$$

where the matrix

$$\tilde{H}_{k+1|k} = \alpha^2 H_{k+1|k}.$$

The number $\alpha > 1$ is chosen in such a way that the set $\tilde{E}_{k+1|k} \cap \hat{X}_{k+1} \neq \emptyset$, and it should contain some sphere of non-zero radius. Formulas for selecting α and necessary explanations are given here [44,45]. An ellipsoid E_{k+1} covering the intersection $\tilde{E}_{k+1|k} \cap \hat{X}_{k+1}$ can be obtained using standard iterative procedures [52, 55, 56]. In this paper, the construction of the ellipsoid E_{k+1} , is carried out iteratively [44] in accordance with the scheme

$$E_{s+1} = [E_s \cap \Pi_{s \bmod N+1, k}]_E \quad s = 0, 1, 2, \dots$$

The ellipsoid $E_{k+1|k}$ is taken as the initial ellipsoid $E_{s=0}$, i.e., $E_{s=0} = E_{k+1|k}$. In this case, the operation of constructing an ellipsoid of minimum volume containing the intersection $E_s \cap \Pi_{s \bmod N+1, k}$ of the ellipsoid E_s and the multidimensional layer $\Pi_{s \bmod N+1, k}$ is used. If it turns out that $E_s \cap \Pi_{s \bmod N+1, k} = \emptyset$ for some s , then matrix H_s of the ellipsoid E_s is multiplied by the factor α_s^2 , which ensures the “immersion” of the ellipsoid E_s into the multidimensional layer $\Pi_{s \bmod N+1, k}$ to a depth of δ (the value δ is the algorithm parameter). The process of constructing ellip-

soids $E_s = E(x_s, H_s)$ will stop [44] at some finite $s = S$. In this case, the inclusion $x_s \in \bigcap_{j=1}^N \Pi_{j,k}$ is true for the center of the resulting ellipsoid $E_s = E(x_s, H_s)$. Finally, we take $E_{k+1} = E_s$.

Note that in the notation (36) and (37) the quantity $\Delta x = x - \hat{x}_{k+1|k}$ appears as a variable. Therefore, the above algorithm can be considered as searching for an increment $\Delta x_{k+1} = \hat{x}_{k+1} - \hat{x}_{k+1|k}$.

2.3. Linearization of the basic equations.

2.3.1. Additive and multiplicative form of quaternion increment. Suppose we have some unknown quaternion q and its estimate \hat{q} . Then we can write that

$$q = \hat{q} + \Delta q_a \text{ or } q = \Delta q \circ \hat{q}, \quad (38)$$

where Δq_a and Δq are estimation errors of \hat{q} . The first representation is called the additive form of the quaternion increment representation; the second is called the multiplicative one [30,33]. The disadvantage of the first form is the fact that if quaternion \hat{q} and increment Δq_a are normalized, their sum is not, and it is necessary to carry out the normalization procedure. If, for example, Δq_a was determined as a result of some estimation algorithm, in which increments of other quantities were also determined, then such normalization in some cases leads to the need for iterative refinement of Δq_a . In the multiplicative form, the result of their multiplication will also be a normalized quaternion. In addition, if we assume that the quaternion Δq is small, i.e., it defines a rotation for a small angle ϕ ($\phi \approx 0$) around some unknown rotation axis defined by a unit vector e , $\|e\|=1$, then, in accordance with the representation of a quaternion in the form (10), the following estimates will hold for its scalar Δq_0 and vector parts Δq_v ,

$$\Delta q_0 \approx 1, \quad \|\Delta q_v\| \approx 0. \quad (39)$$

Moreover, knowing the vector part Δq_v , one can determine the scalar part from the normalization condition in accordance with the following expression

$$\Delta q_0 = \sqrt{1 - \|\Delta q_v\|^2} \quad (40)$$

and hence the quaternion Δq is fully characterized by its vector part. Obviously, all of the above applies equally to the following representation of the quaternion

$$q = \hat{q} \circ \Delta q. \quad (41)$$

Since the quaternion multiplication operation is not commutative, the quaternion increments Δq in (38) and in (41) do not coincide.

In expression (8) for the quaternion η , we will use the representation (41) for the quaternion q and the representation

$$\mu = \Delta \mu \circ \hat{\mu}$$

for the quaternion μ in the coordinate basis e_i , $i = 1:3$, similarly to [3,4]. The reason for choosing such representation will be clear from what follows. The use of the vector part of quaternions Δq and $\Delta \mu$ allows us to reduce the dimension of the state vector when estimating, and their normalization is carried out in accordance with the formula (40).

2.3.2. Linearization of dynamic and measurement equations. In accordance with the general approach, the predicted estimate of the state vector $\hat{x}_{k+1|k}$ is calculated by numerically integrating equations (7), (14)–(16), (18), (20) over the interval $[t_k, t_{k+1}]$ under the initial condition $\tilde{x}(t_k) = \hat{x}_k$, where \hat{x}_k is the state vector estimate obtained at time k . When using the vector part Δq_v and $\Delta \mu_v$ to specify quaternion increments, the increment vector $\Delta x = (\Delta \omega^T, \Delta q^T, \Delta p^T, \Delta r_T^T, \Delta \rho^T, \Delta \mu^T)^T \in R^{19}$ of the state vector, is uniquely characterized by the truncated vector of smaller dimension

$$\delta x = (\Delta \omega^T, \Delta q_v^T, \Delta p^T, \Delta r_T^T, \Delta \rho^T, \Delta \mu_v^T)^T \in R^{17}. \quad (42)$$

Therefore, to calculate at time $(k+1)$ a correction increment Δx_{k+1} for evaluation $\hat{x}_{k+1|k}$ in accordance with the measurement results, it is sufficient to know δx_{k+1} only.

We obtain a linear differential equation that approximately describes the evolution of the increment vector δx . For equations (14), assuming

$$\omega(t) = \tilde{\omega}(t) + \Delta \omega(t), \quad p(t) = \tilde{p}(t) + \Delta p(t),$$

we get in matrix notations

$$\Delta \dot{\omega} = A_\omega(\tilde{\omega}, \tilde{p}) \Delta \omega + A_p(\tilde{\omega}, \tilde{p}) \Delta p. \quad (43)$$

Here, matrices

$$A_\omega(\omega, p) = \begin{pmatrix} 0 & p_1^{-1}(p_2 - 1)\omega_3 & p_1^{-1}(p_2 - 1)\omega_2 \\ p_2^{-1}(1 - p_1)\omega_3 & 0 & p_2^{-1}(1 - p_1)\omega_1 \\ (p_1 - p_2)\omega_2 & (p_1 - p_2)\omega_1 & 0 \end{pmatrix},$$

$$A_p(\omega, p) = \begin{pmatrix} -p_1^{-2}(p_2 - 1)\omega_2\omega_3 & p_1^{-1}\omega_2\omega_3 \\ -p_2^{-1}\omega_1\omega_3 & -p_2^{-2}(1 - p_1)\omega_1\omega_3 \\ \omega_1\omega_2 & -\omega_1\omega_2 \end{pmatrix}.$$

For equation (15), obviously, we have

$$\Delta \dot{p} = 0. \quad (44)$$

Using equation (16), we obtain a differential equation for Δq_v . From (41), considering \tilde{q} as an estimate of q , we obtain $\Delta q = \tilde{q} \circ q$. Differentiating this expression, we have

$$\Delta \dot{q} = \dot{\tilde{q}} \circ q + \tilde{q} \circ \dot{q}. \quad (45)$$

We get $\dot{\tilde{q}} \circ \tilde{q} + \tilde{q} \circ \dot{\tilde{q}} = 0$, differentiating the identity $\tilde{q} \circ \tilde{q} = 1$. Hence, we have

$$\dot{\tilde{q}} = -\tilde{q} \circ \dot{\tilde{q}} \circ \tilde{q}. \quad (46)$$

By definition

$$\dot{\tilde{q}} = 0.5\tilde{q} \circ \tilde{\omega}. \quad (47)$$

Substituting (47) into (46) and then (46) into (45), taking into account representation (41), we obtain

$$\begin{aligned} \Delta \dot{q} &= \tilde{q} \circ \dot{q} - \tilde{q} \circ \dot{\tilde{q}} \circ \tilde{q} \circ q = \\ &= 0.5\tilde{q} \circ \tilde{q} \circ \Delta q \circ (\tilde{\omega} + \Delta\omega) - 0.5\tilde{q} \circ \tilde{q} \circ \tilde{\omega} \circ \tilde{q} \circ \tilde{q} \circ \Delta q = \\ &= 0.5(\Delta q \circ \tilde{\omega} - \tilde{\omega} \circ \Delta q) + 0.5\Delta q \circ \Delta\omega = \\ &= -[\tilde{\omega} \times] \Delta q_v + 0.5\tilde{Q}(\Delta\omega) \Delta q. \end{aligned} \quad (48)$$

Let us estimate the right side of (48). Neglecting the terms of the smallness order higher than the first, using estimates (39) and expression (9) for the matrix $\tilde{Q}(q)$, we obtain

$$\tilde{Q}(\Delta\omega) \Delta q = \begin{pmatrix} 0 & -\Delta\omega^T \\ \Delta\omega & -[\Delta\omega \times] \end{pmatrix} \begin{pmatrix} \Delta q_0 \\ \Delta q_v \end{pmatrix} \approx \begin{pmatrix} 0 \\ \Delta\omega \end{pmatrix}.$$

Taking into account the last equality, from (48) we obtain

$$\Delta \dot{q}_v \approx -[\tilde{\omega} \times] \Delta q_v + 0.5\Delta\omega, \quad \Delta \dot{q}_0 \approx 0. \quad (49)$$

For the remaining constant parameters ρ , r_T , and μ , one can obtain the following equations

$$\Delta \dot{\rho} = 0, \quad \Delta \dot{r}_T = 0, \quad \Delta \dot{\mu}_v = 0. \quad (50)$$

Combining equations (43), (44), (49), and (50), we obtain an equation describing the change in time of the vector δx in the linear approximation

$$\delta \dot{x} = \begin{pmatrix} A(\tilde{\omega}, \tilde{p}) & \Theta_{8 \times 9} \\ \Theta_{9 \times 8} & \Theta_{9 \times 9} \end{pmatrix} \delta x, \quad (51)$$

where 8×8 -matrix

$$A(\omega, p) = \begin{pmatrix} A_\omega(\omega, p) & \Theta_{3 \times 3} & A_p(\omega, p) \\ 0.5I_3 & -[\omega \times] & \Theta_{3 \times 2} \\ \Theta_{2 \times 3} & \Theta_{2 \times 3} & \Theta_{2 \times 2} \end{pmatrix}.$$

Let us assume that at time moment t_k vector

$$\delta x(t_k) = \delta x_k \in \delta E_k = E(0, H_k).$$

Then, in accordance with the approach described in Section 2.2, for the matrix A_{k+1} used in calculating the matrix $H_{k+1|k}$ of ellipsoid $\delta E_{k+1|k} = E(0, H_{k+1|k})$ by virtue of (51) and (35), we take the following expression

$$A_{k+1} = \begin{pmatrix} \exp(A_{k+1/2} \Delta) & \Theta_{8 \times 9} \\ \Theta_{9 \times 8} & I_9 \end{pmatrix}, \quad (52)$$

Here, $A_{k+1/2} = A(\hat{\omega}_{k+1/2}, \hat{p}_k)$, $\hat{\omega}_{k+1/2} = 0.5(\hat{\omega}_{k+1|k} + \hat{\omega}_k)$.

The ellipsoid $\delta E_{k+1|k}$ ($\delta E_{k+1|k} \subset R^{17}$) contains the possible values of the vector $\delta x_{k+1|k}$.

Let us linearize the functions $g_j(x)$, appearing in the measurement equations (23) and (24), at a point $\hat{x}_{k+1|k}$ with respect to the vector δx . To do this, we substitute the terms of estimates and their increments into the function expressions. The terms linear on δx will contain the required gradients of the functions $g_j(x)$.

For equation (23), considered for the time moment $k+1$, we have

$$\begin{aligned} \tilde{r}_{k+1} &= \hat{r}_{k+1|k} + \Delta r + R(\hat{q}_{k+1|k} \circ \Delta q)(\hat{\rho}_{k+1|k} + \Delta \rho) + \xi_{k+1}^r = \\ &= \hat{r}_{k+1|k} + \Delta r + R(\hat{q}_{k+1|k})R(\Delta q)(\hat{\rho}_{k+1|k} + \Delta \rho) + \xi_{k+1}^r \approx \\ &\approx \hat{r}_{k+1|k} + \Delta r + R(\hat{q}_{k+1|k})(I_3 + 2[\Delta q_v \times])(\hat{\rho}_{k+1|k} + \Delta \rho) + \xi_{k+1}^r \approx \\ &\approx \hat{r}_{k+1|k} + R(\hat{q}_{k+1|k})\hat{\rho}_{k+1|k} + \Delta r + R(\hat{q}_{k+1|k})\Delta \rho - 2R(\hat{q}_{k+1|k}) \times \\ &\quad \times [\hat{\rho}_{k+1|k} \times] \Delta q_v + \xi_{k+1}^r. \end{aligned} \quad (53)$$

When obtaining the last equality, expression (22) for the matrix $R(q)$ and assumption (39) were used.

For equation (24) we get

$$\begin{aligned} \tilde{\eta}_{k+1} &= q_{k+1} \circ \mu_{k+1} + \xi_{k+1}^\eta = \hat{q}_{k+1|k} \circ \Delta q \circ \Delta \mu \circ \hat{\mu}_{k+1|k} + \xi_{k+1}^\eta = \\ &= \hat{q}_{k+1|k} \circ \Delta \eta \circ \hat{\mu}_{k+1|k} + \xi_{k+1}^\eta, \end{aligned} \quad (54)$$

where

$$\Delta \eta = \Delta q \circ \Delta \mu.$$

Using the quaternion multiplication formula (4), assumption (39), and similar assumptions for $\Delta \mu_0$ and $\Delta \mu_v$, we obtain

$$\Delta \eta_0 = \Delta q_0 \cdot \Delta \mu_0 - (\Delta q_v, \Delta \mu_v) \approx \Delta q_0 \cdot \Delta \mu_0 \approx 1,$$

$$\Delta \eta_v = \Delta q_0 \cdot \Delta \mu_v + \Delta \mu_0 \cdot \Delta q_v + \Delta q_v \times \Delta \mu_v \approx \Delta \mu_v + \Delta q_v.$$

Hence,

$$\Delta\eta = \begin{pmatrix} \Delta\eta_0 \\ \Delta\eta_v \end{pmatrix} \approx \begin{pmatrix} 1 \\ \Delta q_v + \Delta\mu_v \end{pmatrix} = \begin{pmatrix} 1 \\ \Theta_{3 \times 1} \end{pmatrix} + \begin{pmatrix} 0 \\ \Delta q_v + \Delta\mu_v \end{pmatrix}.$$

Substituting this expression into (54), we obtain

$$\begin{aligned} \tilde{\eta}_{k+1} &\approx \hat{q}_{k+1|k} \circ \hat{\mu}_{k+1|k} + \hat{q}_{k+1|k} \circ \begin{pmatrix} 0 \\ \Delta q_v + \Delta\mu_v \end{pmatrix} \circ \hat{\mu}_{k+1|k} + \xi_{k+1}^\eta = \\ &= \hat{q}_{k+1|k} \circ \hat{\mu}_{k+1|k} + Q(\hat{q}_{k+1|k}) \bar{Q}(\hat{\mu}_{k+1|k}) \begin{pmatrix} 0 \\ \Delta q_v + \Delta\mu_v \end{pmatrix} + \xi_{k+1}^\eta = \\ &= \hat{\mu}_{k+1|k} \circ \hat{q}_{k+1|k} + \Gamma(\hat{q}_{k+1|k}, \hat{\mu}_{k+1|k}) \Delta q_v + \\ &\quad + \Gamma(\hat{q}_{k+1|k}, \hat{\mu}_{k+1|k}) \Delta \mu_v + \xi_{k+1}^\eta, \end{aligned} \quad (55)$$

where 4×3 -matrix

$$\Gamma(q, \mu) = \begin{pmatrix} -q_0 \mu_v^T - \mu_0 q_v^T - ([\mu_v \times] q_v)^T \\ \mu_0 q_0 I_3 + \mu_0 [q_v \times] - q_0 [\mu_v \times] - [q_v \times] [\mu_v \times] - q_v \mu_v^T \end{pmatrix}.$$

From expressions (53), (55) and restrictions on measurement noise, we obtain that the components of the increment vector δx must satisfy the following 7 inequalities

$$\begin{aligned} &\| \tilde{r}_{k+1} - \hat{r}_{k+1|k} - R(\hat{q}_{k+1|k}) \hat{\rho}_{k+1|k} - \Delta r - R(\hat{q}_{k+1|k}) \Delta \rho + \\ &\quad + 2R(\hat{q}_{k+1|k}) [\hat{\rho}_{k+1|k} \times] \Delta q_v \|_\infty \leq c^r, \\ &\| \tilde{\eta}_{k+1} - \hat{q}_{k+1|k} \circ \hat{\mu}_{k+1|k} - \Gamma(\hat{q}_{k+1|k}, \hat{\mu}_{k+1|k}) \Delta q_v - \\ &\quad - \Gamma(\hat{q}_{k+1|k}, \hat{\mu}_{k+1|k}) \Delta \mu_v \|_\infty \leq c^\eta. \end{aligned} \quad (56)$$

These inequalities can be rewritten in the following standard form

$$\| \Delta y_{k+1}^r - H_{r,k+1} \delta x \|_\infty \leq c^r, \quad (57)$$

$$\| \Delta y_{k+1}^\eta - H_{\eta,k+1} \delta x \|_\infty \leq c^\eta. \quad (58)$$

Here,

$$\begin{aligned} \Delta y_{k+1}^r &= \tilde{r}_{k+1} - \hat{r}_{k+1|k} - R(\hat{q}_{k+1|k}) \hat{\rho}_{k+1|k}, \\ H_{r,k+1} &= [\Theta_{3 \times 3} \quad -2R(\hat{q}_{k+1|k}) [\hat{\rho}_{k+1|k} \times] \quad \Theta_{3 \times 2} \\ &\quad I_3 \quad R(\hat{q}_{k+1|k}) \quad \Theta_{3 \times 3}], \\ \Delta y_{k+1}^\eta &= \tilde{\eta}_{k+1} - \hat{q}_{k+1|k} \circ \hat{\mu}_{k+1|k}, \\ H_{\eta,k+1} &= [\Theta_{4 \times 3} \quad \Gamma(\hat{q}_{k+1|k}, \hat{\mu}_{k+1|k}) \quad \Theta_{4 \times 2} \\ &\quad \Theta_{4 \times 3} \quad \Theta_{4 \times 3} \quad \Gamma(\hat{q}_{k+1|k}, \hat{\mu}_{k+1|k})]. \end{aligned}$$

Note that (56) contains 4 inequalities that must be satisfied using only three variables, namely, by

the vector $\Delta q_v + \Delta \mu_v$ of dimension 3. In the general case, these inequalities may turn out to be inconsistent, i.e., the solution area may be empty. Therefore, at the numerical solution, when finding the intersection with the ellipsoid, three of these four inequalities were chosen, but in such a way that the discrepancy for the not considered inequality was minimal.

2.4. Problem solution algorithm. We consider the estimate of the state vector \hat{x}_k and the matrix $H_k = H_k^T > 0$ of the ellipsoid δE_k to be known. Let us describe the procedure for calculating the estimate \hat{x}_{k+1} .

1. Numerically integrate equations (14) and (16) in real time on the interval $[t_k, t_{k+1}]$ under the initial condition \hat{x}_k to calculate estimates $\hat{\omega}_{k+1|k}$ and $\hat{q}_{k+1|k}$. For the remaining components of the state vector, we assume $\hat{\mu}_{k+1|k} = \hat{\mu}_k$, $\hat{p}_{k+1|k} = \hat{p}_k$, $\hat{\rho}_{k+1|k} = \hat{\rho}_k$, and $\hat{r}_{T,k+1|k} = \hat{r}_{T,k}$.

2. At the time moment t_{k+1} , we calculate the matrix A_{k+1} in accordance with (52) and the matrix $H_{k+1|k}$ of the ellipsoid $\delta E_{k+1|k}$.

3. An ellipsoid $\delta E_{k+1}(\delta \hat{x}_{k+1}, H_{k+1})$ is constructed that contains the intersection of the ellipsoid $\delta E_{k+1|k}$ and the layers corresponding to inequalities (57) and (58), taken for the time moment $k+1$, as proposed in subsection 2.2. The center of the obtained ellipsoid δE_{k+1} , vector $\delta \hat{x}_{k+1}$ (in the general case $\delta \hat{x}_{k+1} \neq 0$) will satisfy the linearized inequalities (57) and (58).

4. Using increment vector

$$\delta \hat{x}_{k+1} = (\Delta \hat{\omega}_{k+1}^T, \Delta \hat{q}_{v,k+1}^T, \Delta \hat{p}_{k+1}^T, \Delta \hat{r}_{T,k+1}^T, \Delta \hat{\rho}_{k+1}^T, \Delta \hat{\mu}_{v,k+1}^T)^T,$$

calculate the vector

$$\hat{x}_{k+1} = (\hat{\omega}_{k+1}^T, \hat{q}_{k+1}^T, \hat{p}_{k+1}^T, \hat{r}_{T,k+1}^T, \hat{\rho}_{k+1}^T, \hat{\mu}_{k+1}^T)^T$$

according to the following formulas:

$$\begin{aligned} \hat{\omega}_{k+1} &= \hat{\omega}_{k+1|k} + \Delta \hat{\omega}_{k+1}, \\ \hat{p}_{k+1} &= \hat{p}_{k+1|k} + \Delta \hat{p}_{k+1}, \\ \hat{r}_{T,k+1} &= \hat{r}_{T,k+1|k} + \Delta \hat{r}_{T,k+1}, \\ \hat{\rho}_{k+1} &= \hat{\rho}_{k+1|k} + \Delta \hat{\rho}_{k+1}. \end{aligned}$$

The quaternion \hat{q}_{k+1} is calculated as follows:

$$\hat{q}_{k+1} = \hat{q}_{k+1|k} \circ \Delta \hat{q}_{k+1} = Q(\hat{q}_{k+1|k}) \Delta \hat{q}_{k+1},$$

where

$$\Delta \hat{q}_{k+1} = (\Delta \hat{q}_{0,k+1}, \Delta \hat{q}_{v,k+1}^T)^T,$$

$$\Delta \hat{q}_{0,k+1} = \sqrt{1 - \|\Delta \hat{q}_{v,k+1}\|^2}.$$

The quaternion $\hat{\mu}_{k+1}$ is calculated similarly:

$$\hat{\mu}_{k+1} = \Delta\hat{\mu}_{k+1} \circ \hat{\mu}_{k+1|k} = \bar{Q}(\hat{\mu}_{k+1|k})\Delta\hat{\mu}_{k+1},$$

where

$$\Delta\hat{\mu}_{k+1} = (\Delta\hat{\mu}_{0,k+1}, \Delta\hat{\mu}_{v,k+1}^T)^T,$$

$$\Delta\hat{\mu}_{0,k+1} = \sqrt{1 - \|\Delta\hat{\mu}_{v,k+1}\|^2}.$$

5. The increment vector $\delta\hat{x}_{k+1}$ was used for calculation of the vector \hat{x}_{k+1} . So, we set $\delta E_{k+1} = E(0, H_{k+1})$.

The estimation process will stop when $\delta\hat{x}_{k+1} = 0$, i.e., when the calculated estimates, i.e., the vector $\hat{x}_{k+1|k}$ will satisfy the inequalities (57) and (58) associated with measurements.

The properties of the described algorithm were studied using numerical simulation.

3. NUMERICAL SIMULATION OF THE ALGORITHM FOR ESTIMATING THE RELATIVE POSITION OF THE SATELLITE

The data from [3] were taken as a model example. The principal moments of inertia of the satellite were $J_1 = 4.0 \text{ kgm}^2$, $J_2 = 8.0 \text{ kgm}^2$, $J_3 = 5.0 \text{ kgm}^2$. The simulation of the estimation algorithm was carried out for different initial values of the angular velocity vector $\omega(t_0)$, whose components $\omega_j(t_0)$, $j = 1:3$, were chosen randomly from the interval $[-1, 1]$ rad/sec. The initial attitude quaternion $q(t_0)$ of the NSC principal inertia axes relative to the inertial reference frame was chosen in a similar way. Its components $q_j(t_0)$, $j = 0:3$, were selected from the interval $[-1, 1]$. The resulting quaternion was normalized. The constant quaternion μ of the orientation of the graphical reference frame relative to the principal reference frame was chosen in the same way. The position of the graphical reference frame in the NSC principal reference frame was given by the vector $\rho = (0.15, 0.0, 0.0)^T$. The position of the origin of the principal reference frame in the inertial reference frame was characterized by a constant vector $r_T = (10.0, 1.0, 2.0)^T$. These values were considered unknown and were used when integrating equations (14) and (16) to calculate the so-called true values of these parameters and to form the measured values of the distance \tilde{r}_k and $\tilde{\eta}_k$. Measurement noises ξ_k^r and ξ_k^η were generated as a random process of the white noise type, uniformly distributed in the intervals $[-c^r, c^r]$ and $[-c^\eta, c^\eta]$, respectively. The maxi-

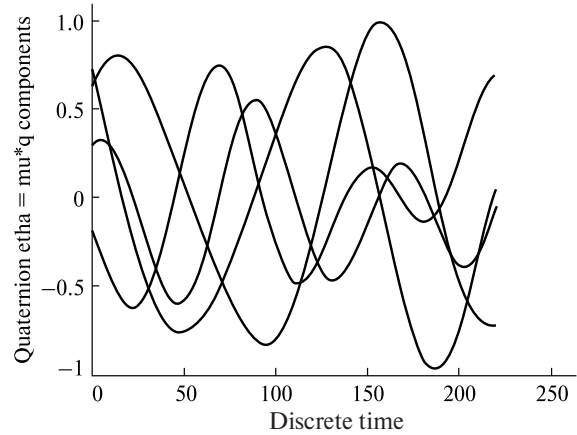


Figure 2. Variation in time of the components of the attitude quaternion of the graphical reference frame

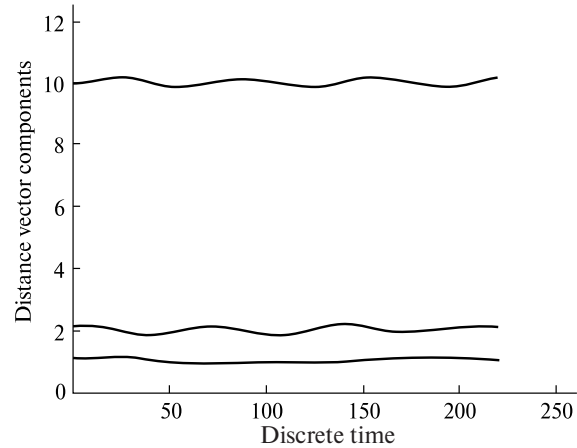


Figure 3. Variation in time of the components of the distance vector to the origin of the graphical reference frame

imum values of measurement noise are $c^r = 0.02 \text{ m}$ and $c^\eta = 0.06$, which corresponds to the accuracy of determining the position of 2 cm and orientation within 3° of the Euler angles. The measurement period Δ was chosen to be proportional to the norm of the initial angular velocity vector with a step of 0.5 seconds. The duration of the estimation process was 220 discrete time cycles.

Plots of the coordinates of the attitude quaternion $\eta(t)$, as well as the components of the distance vector $r(t)$ at the initial values of the angular velocity $\omega(t_0) = (0.09, -0.05, 0.04)^T$ and the attitude quaternion $q(t_0) = (0.1005, 0.5025, 0.3015, 0.8040)^T$, are shown in Fig. 2 and 3, respectively. It was chosen

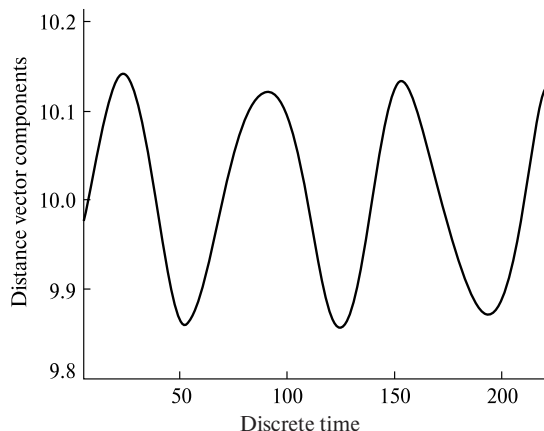


Figure 4. Change in time of the 1-st component of the vector $r(t)$

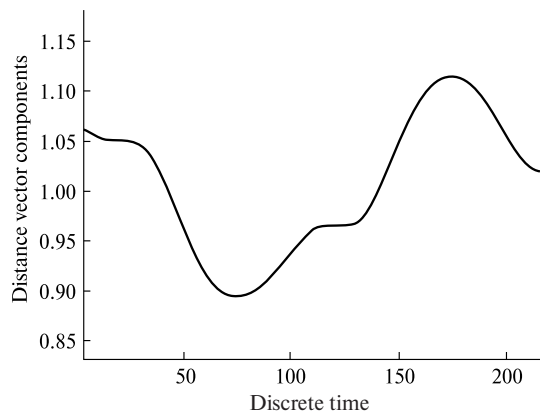


Figure 5. Change in time of the 3-rd component of the vector $r(t)$

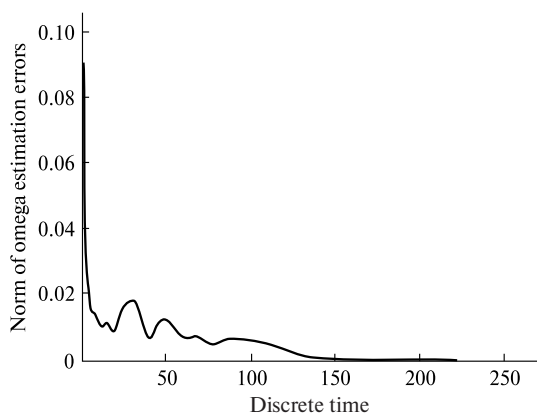


Figure 6. Variation in time of angular velocity estimation error $e_k^\omega = \|\omega(t_k) - \hat{\omega}_k\|_\infty$

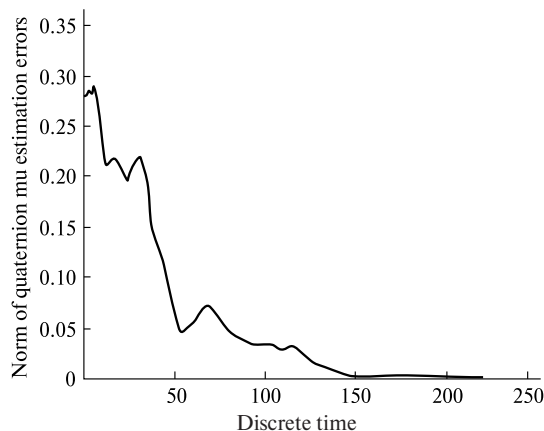


Figure 7. Variation in time of quaternion estimation error $e_k^q = \|q(t_k) - \hat{q}_k\|_\infty$

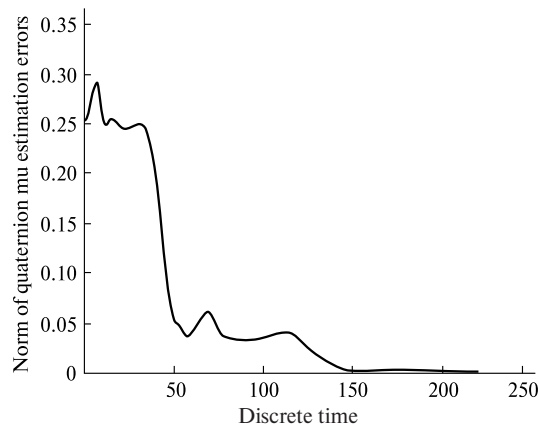


Figure 8. Variation in time of quaternion estimation error $e_k^\mu = \|\mu - \hat{\mu}_k\|_\infty$

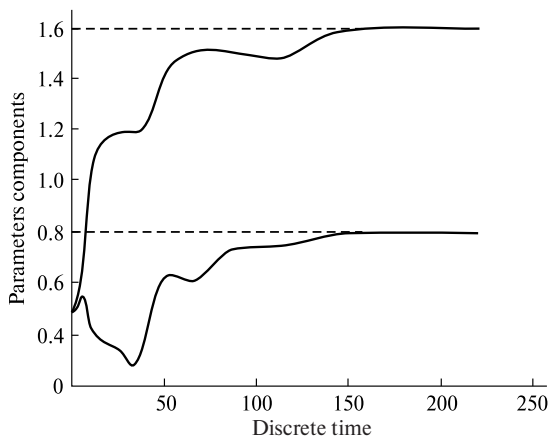


Figure 9. Change of parameter estimates $\hat{p}_{1,k}$ and $\hat{p}_{2,k}$ with time

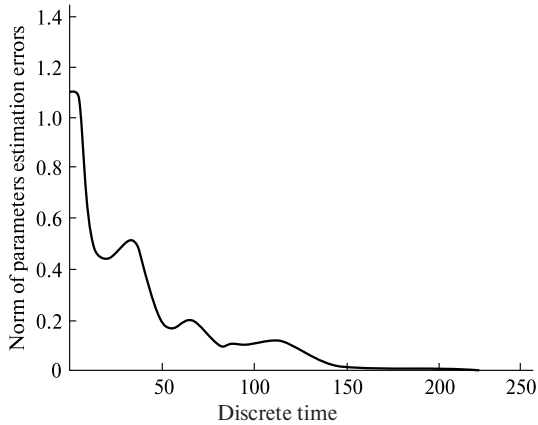


Figure 10. Time variation of parameter estimation error $e_k^p = \|\hat{p}^* - \hat{p}_k\|_\infty$

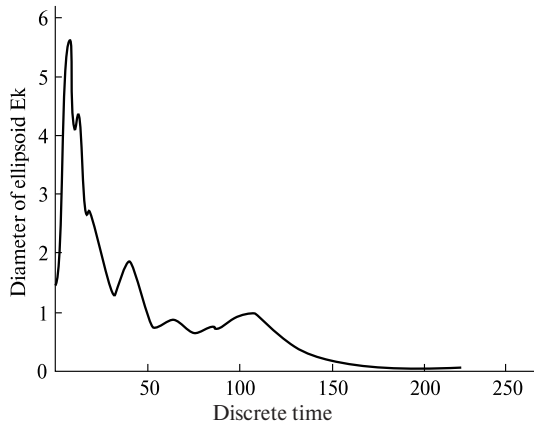


Figure 11. Change in time of the norm of matrix H_k of the ellipsoid δE_k

$H_0 = 1 \cdot I$ and $\Delta = 1$ sec in this example. The initial estimate of the quaternion were $\hat{\mu}_0 = (1, 0, 0, 0)^T$, $\hat{q}_0 = \tilde{\eta}_0$, $\hat{r}_{T,0} = \tilde{r}_0$. The initial estimate of the moment inertia ratio vector was $\hat{p}_0 = (\hat{p}_{1,0}, \hat{p}_{2,0})^T = (0.5, 0.5)^T$. The remaining elements of the vector \hat{x}_0 were chosen to be zero. The true values of the inertia moment ratios were the following $p_1^* = J_1 J_3^{-1} = 0.8$, $p_2^* = J_2 J_3^{-1} = 1.6$, i.e., the true vector of parameters $p^* = (p_1^*, p_2^*)^T = (0.8, 1.6)^T$.

The relatively small change of the distance vector components is due to the small value of the vector ρ . This change is rather complex, as shown in Fig. 4 and 5, which show the change of the first component in Fig. 4 and the third one in Fig. 5.

This is due to the fact that the initial conditions for the angular velocity were such that the coordinates of the angular velocity vector in the NSC principal reference frame do not remain constant. This means that the angular velocity vector changes its position relative to this frame and, therefore, in the considered case, the free rotation of the NSC is not rotation around the fixed axis.

Estimation errors of the NSC angular velocity vector, $e_k^\omega = \|\omega(t_k) - \hat{\omega}_k\|_\infty$ and the NSC attitude quaternion $e_k^q = \|q(t_k) - \hat{q}_k\|_\infty$ at discrete times $t_k = k \cdot \Delta t$ obtained by the proposed estimation algorithm, are shown in Fig. 6 and Fig. 7, respectively.

The angular velocity estimation error at the end of the algorithm operation interval did not exceed 0.0003 rad/sec, which is no more than 0.3 % of the nominal value. The estimation accuracy of quaternions $q(t)$ and μ at the end of the estimation process reached the value of 0.004. The plot of the estimation error of the quaternion μ and the change of the parameter estimates $\hat{p}_{1,k}$ and $\hat{p}_{2,k}$ with time are shown in Fig. 8 and 9, respectively.

The change of the estimation error $e_k^p = \|\hat{p}^* - \hat{p}_k\|_\infty$ of the vector of the NSC inertia moments ratios is shown in Fig. 10. The steady value of the estimation error did not exceed 0.003.

The plot of the norm $\|H_k\|_2 = \sqrt{\lambda_k^{\max}}$ of matrix H_k of the ellipsoid δE_k , where λ_k^{\max} is the maximum eigenvalue of the matrix H_k , is shown in Fig. 11. From the consideration of transient processes in Fig. 6–10 it follows that the time of the transient process does not exceed 180 cycles, in the case under consideration it is 180 seconds, i.e., 3 minutes.

4. CONCLUSIONS

The results of the numerical simulation showed the operability and efficiency of using the proposed ellipsoidal filter in solving the estimation problem of parameters of the NSC relative rotational motion. As it follows from the simulation results, the use of the proposed estimation technique allows not only increase the accuracy of the measured parameters (distance vector and attitude quaternion) by order of magnitude but also to obtain rather accurate estimates of all other motion parameters. In this paper, we deliberately considered a simplified case in which the measuring device remained stationary

since it was necessary to find out the fundamental possibility of using the ellipsoidal estimation method to solve the formulated problem. To consider the case when the measuring device is also installed on a spacecraft that can perform maneuvers near the NSC, it is necessary to use additionally the equations of the relative orbital motion of the two spacecrafts.

There are a number of questions related to the application of the proposed estimation algorithm. Namely, the determination of the areas of initial values of the motion of the NSC, at which the algorithm

converges, the choice of the algorithm parameters, etc., are planned to be considered in the course of continuing this work. The information provided by the algorithm is necessary for planning the SSC rendezvous and capture trajectories in compliance with safety requirements.

This work contains results of the project No. 09/22/2 funded in a framework of the “Target Comprehensive Program of the National Academy of Sciences of Ukraine for Scientific Space Research in 2018-2022”.

REFERENCES

1. Aghili F., Kuryllo M., Okouneva G., English Ch. (2011). Fault-tolerant position/attitude estimation of free-floating space objects using a laser range sensor. *IEEE Sensors J.*, **11**, № 1, 176—185.
2. Aghili F., Su C. (2016). Robust relative navigation by integration of ICP and adaptive Kalman filter using laser scanner and IMU. *IEEE/ASME Transactions on Mechatronics*, **21**, № 4, 2015—2026. DOI: 10.1109/TMECH.2016.2547905.
3. Aghili F. (2012). A prediction and motion-planning scheme for visually guided robotic capturing of free-floating tumbling objects with uncertain dynamics. *IEEE Transactions on Robotics*, **28**, № 3, 634—649.
4. Aghili F., Parsa K. (2009). Motion and parameter estimation of space objects using laser-vision data. *J. Guidance, Control, and Dynamics*, **32**, № 2, 537—549. DOI: 10.2514/1.37129.
5. Aghili F. (2010). Automated rendezvous & docking without impact using a reliable 3D vision system. *Guidance, Navigation, and Control Conference*, 2-5 August 2010, Toronto, Ontario Canada. <https://doi.org/10.2514/6.2010-7602>
6. Amel'kin N. I. (2012). *Rigid body dynamics*. Moscow: MIPT, 80 p. URL: https://studylib.ru/doc/1678659/n.i.-amel._kin-dinamika-tverdogo-tela (Last accessed: 01.02.2023). [in Russian].
7. Arulampalam M. S., Maskell S., Gordon N., Clapp T. (2002). A tutorial on particle filters for online nonlinear/non-Gaussian bayesian tracking. *IEEE Transactions on Signal processing*, **50**, № 2, 174—188.
8. Balahoncov V. G., Ivanov V. A., Shabanov V. I. (1973). *Approaching in space*. Moscow: Voenizdat, 240 p. [in Russian].
9. Blanchini F., Miani S. (2015). *Set-theoretic methods in control*. Switzerland: Springer International Publishing.
10. Bragazin A. F. (2018). *Control of spacecraft approaching (navigation, guidance, motion correction)*. Koroljov: RKK “Jener-gija”, 470 p. [in Russian].
11. Capuano V., Kim K., Hu J., Harvard A., Chung S. (2018). Monocular-based pose determination of uncooperative known and unknown space objects. *Proceedings of the 69th International Astronautical Congress (IAC)*. Bremen, Germany, 1-5 October 2018.
12. Chabane S. B., Maniu C. S., Alamo T., Camacho E. F., Dumur D. (2014). A new approach for guaranteed ellipsoidal state estimation. *Preprints of the 19th World Congress. The International Federation of Automatic Control*. Cape Town, South Africa. August 24—29, 2014. pp. 6533—6538.
13. Cheng Y., Crassidis J. L. (2010). Particle filtering for attitude estimation using a minimal local-error representation. *J. Guidance, Control, and Dynamics*, **33**, № 4, 1305—1310. <https://doi.org/10.2514/1.47236>
14. Chernousko F. L. (1994). *State estimation for dynamic systems*. Boca Raton: CRC Press.
15. Crassidis J. L., Markley F. L., Cheng Y. (2007). Survey of nonlinear attitude estimation methods. *J. Guidance, Control and Dynamics*, **30**, No. 1, 12—28. <https://doi.org/10.2514/1.22452>
16. D'Amico S., Benn M., Jrgensen J. L. (2014). Pose estimation of an uncooperative spacecraft from actual space imagery. *Int. J. Space Science and Engineering*, **2**, № 2, 171—189. DOI: 10.1504/IJSPACESE.2014.060600
17. Dementhon D. F., Davis L. S. (1995). Model-based object pose in 25 lines of code. *International J. Computer Vision*, **15**, 123—141. <https://doi.org/10.1007/BF01450852>.
18. Espinoza A. T., Setterfield T. P. (2019). Point-to-CAD 3D registration algorithm for relative navigation using depth-based maps. 2019 IEEE Aerospace Conference, 1—7. DOI: 10.1109/AERO.2019.8742148.
19. Farrell J. A. (2008). *Aided navigation. GPS with high rate sensors*. New York: The McGraw-Hill Companies, 553 p.
20. Fehse W. (2003). *Automated rendezvous and docking of spacecraft*. Cambridge: Cambridge University Press, 517 p.

21. Grishin V. A., Zhukov B. S. (2020). Peculiarities of image recognition at its application to relative navigation tasks at spacecraft docking. *Modern problems of Earth Remote Control*, **17**, № 7, 58—66 [in Russian].
22. Gubarev V., Salnikov N., Melnychuk S., Shevchenko V., Maksymyuk L. (2021). Special cases in determining the spacecraft position and attitude using computer vision system. *Chapter 10 in the book "Advanced Control Systems: Theory and Applications"*. River Publishers Series in Automation, Control and Robotics. pp. 289—316.
23. Ivanov D. S., Karpenko S. O., Ovchinnikov M. Ju., Sakovich M. A. (2012). Relative motion determination of satellites at their separation on results of videoimages processing. *Preprints of Keldysh IAM*. № 057, 24 p.
24. *Kalman Filtering and Neural Networks* (2001). (edited by S. Haykin). New York, Toronto: John Wiley&Sons, Inc., 284 p.
25. Kelsey J. M., Byrne J., Cosgrove M., Seereeram S., Mehra R. K. (2006). Vision-based relative pose estimation for autonomous rendezvous and docking. *2006 IEEE Aerospace Conference*. pp. 20—39. DOI: 10.1109/AERO.2006.1655916.
26. Koshkin N., Melikyants S., Korobeinikova E., Shakun L., Strakhova S., Kashuba V., Romanyuk Ya., Terpan S. (2019). Simulation of the orbiting spacecraft to analysis and understand their rotation based on photometry. *Odessa Astronomical Publications*, **32**, 158—161. DOI: <http://dx.doi.org/10.18524/1810-4215.2019.32.183899>.
27. Koshkin N., Shakun L., Kozhukhov O., Kozhukhov D., Mamarev V., Prysiaznyi V., Ozeryan A., Bilinsky A., Kudak V., Neubauer I. (2021). Simultaneous multi-site photometry of leo satellites for rotation characterization. *Proceedings of the 8th European Conference on Space Debris*. Darmstadt, Germany, 20—23 April 2021. <http://conference.sdo.esoc.esa.int>.
28. Kuntzevich V. M., Lychak M. (1981). *Guaranteed Estimates, Adaptation and Robustness in Control Systems*. Berlin, New York: Springer-Verlag.
29. Kurzhanski A. B., Valyi I. (1997). *Ellipsoidal Calculus for Estimation and Control*. Boston: Birkhauser.
30. Leffens E. J., Markley F. L., Shuster M. D. (1982). Kalman filtering for spacecraft attitude estimation. *J. Guidance*, **5**, № 5, 417—429.
31. Liang H., Wang J., Wang Y., Huo W. (2020). Monocular-vision-based spacecraft relative state estimation under dual number algebra. *Proceedings of the Institution of Mechanical Engineers, Part G: J. Aerospace Engineering*, **234**, 221—235. DOI:10.1177/0954410019864754.
32. Markley F. L., Crassidis J. L. (2014). *Fundamentals of spacecraft attitude determination and control*. New York: Springer Science+Business Media.
33. Markley F. L. (2003). *Multiplicative versus additive filtering for spacecraft attitude determination*. URL: <https://ntrs.nasa.gov/citations/20040037784>. (Last accessed 01.02.2023).
34. Masutani Y., Iwatsu T., Miyazaki F. (1994). Motion estimation of unknown rigid body under no external forces and moments. *Proceedings of the 1994 IEEE International Conference on Robotics and Automation*, **2**, 1066—1072. doi: 10.1109/ROBOT.1994.351227.
35. Moghaddam B. M., Chhabra R. (2021). On the guidance, navigation and control of in-orbit space robotic missions: A survey and prospective vision. *Acta Astronautica*, **184**, 70—100. <https://doi.org/10.1016/j.actaastro.2021.03.029>.
36. Molina Saqui J. C., Tkachev S. S. (2021). Kalman filter application for the angular motion estimation by video processing. *Keldysh IAM Preprints*, № 27, 27 p. <https://doi.org/10.20948/prepr-2021-27-e>
37. Nocerino A., Opromolla R., Fasano G., Grassi M. (2021). LIDAR-based multi-step approach for relative state and inertia parameters determination of an uncooperative target. *Acta Astronautica*, **181**, 662—678. <https://doi.org/10.1016/j.actaastro.2021.02.019>
38. Opromolla R., Fasano G., Rufino G., Grassi M. (2017). A review of cooperative and uncooperative spacecraft pose determination techniques for close proximity operations. *Progress in Aerospace Sciences*, **93**, 53—72.
39. Opromolla R., Nocerino A. (2019). Uncooperative spacecraft relative navigation with lidar-based unscented Kalman filter. *IEEE Access*, **7**, 180012—180026. DOI: 10.1109/ACCESS.2019.2959438.
40. Oumer N. W., Panin G. (2012). Tracking and pose estimation of non-cooperative satellite for on-orbit servicing. *Proceedings of the conference i-SAIRAS 2012. European Space Agency (ESA). i-SAIRAS*. 4-6 Sep 2012, Turin, Italy.
41. Pontrjagin L. S. (1982). *Ordinary differential equations*. Moscow: Nauka, 332 p. [in Russian].
42. Poznyak A., Polyakov A., Azhmyakov V. (2014). *Attractive ellipsoids in robust control*. Switzerland: Springer International Publishing.
43. Salnikov N. N., Melnychuk S. V., Gubarev V. F. (2018). Ellipsoidal pose estimation of an uncooperative spacecraft from video image data. *in book "Control Systems: Theory and Applications"*. River Publishers Series in Automation, Control and Robotics, 169—195.
44. Salnikov N. N. (2012). On one modification of linear regression estimation algorithm using ellipsoids. *J. Automation and Information Sci.*, **44**, № 3, 15—32.
45. Salnikov N. N. (2014). Estimation of State and Parameters of Dynamic System with the Use of Ellipsoids at the Lack of a Priori Information on Estimated Quantities. *J. Automation and Information Sci.*, **46**, № 4, 60—75.

46. Sarychev V. A., Paglione P., Guerman A. D. (2008). Stability of equilibria for a satellite subject to gravitational and constant torques. *J. Guidance Control and Dynamics*, **31**, № 2, 386—394.
47. Savchuk A.P., Fokov A.A. (2018). Determination of non-cooperative object parameters in orbital service tasks. *Technical Mechanics*, № 4, 30—45 [in Russian].
48. Schweppe F. C. (1973). *Uncertain dynamic systems*. Englewood Cliffs, N.J., Prentice-Hall, 563 p.
49. Segal S., Carmi A., Gurfil P. (2011). Vision-based relative state estimation of non-cooperative spacecraft under modeling uncertainty. *Aerospace Conference*. Piscataway (NJ): IEEE Publ., 1—8. DOI:10.1109/AERO.2011.5747479.
50. Shi J.-F., Ulrich S., Ruel S. (2017). Spacecraft pose estimation using principal component analysis and a monocular camera. *AIAA Guidance, Navigation, and Control Conference*. Grapevine, Texas, 9—13 January 2017, 1034.
51. Shijie Zh., Fenghua L., Xibin C., Liang H. (2010). Monocular vision-based two-stage iterative algorithm for relative position and attitude estimation of docking spacecraft. *Chinese J. Aeronautics*, **23**, № 2, 204—210.
52. Shor N. 3., Stecenko S. I. (1989). *Quadratic extremal problems and non-differential optimization*. Kiev: Naukova dumka, 208 p. [in Russian].
53. Stainfeld D., Rock S. M. (2009). Rigid body inertia estimation with applications to the capture of a tumbling satellite. *Proceedings of 19th AAS/AIAA Spaceflight Mechanics Meeting*. Savannah, GA, 343—356.
54. Volosov V., Salnikov N., Melnychuk S., Shevchenko V. (2021). Control synthesis of rotational and spatial spacecraft motion at approaching stage of docking. *Chapter 12 in the book "Advanced Control Systems: Theory and Applications"*. River Publishers Series in Automation, Control and Robotics. 331—364.
55. Volosov V. V., Tyutyunnik L. I. (2000). Development and analysis of robust algorithms for guaranteed ellipsoidal estimation of the state of multidimensional linear discrete dynamic systems. Part 1. *J. Automation and Information Sci.*, **32**, № 3, 37—46.
56. Volosov V. V., Tyutyunnik L. I. (2000). Development and analysis of robust algorithms for guaranteed ellipsoidal estimation of the state of multidimensional linear discrete dynamic systems. Part 2. *J. Automation and Information Sci.*, **32**, № 11, 13—23.
57. Volpe R., Sabatini M., Palmerini G. B. (2017). Pose and shape reconstruction of a noncooperative spacecraft using camera and range measurements. *Int. J. Aerospace Eng.*, **2017**, Article ID 4535316, 13 p. <https://doi.org/10.1155/2017/4535316>.
58. Yu X., Yu F., He Z. (2014). Stereo vision based relative state estimation for non-cooperative spacecraft with outliers. *Proceedings of the 33rd Chinese Control Conference*, 763—769. DOI: 10.1109/ChiCC.2014.6896723.

Стаття надійшла до редакції 16.02.2023

Після доопрацювання 16.02.2023

Прийнято до друку 04.04.2023

Received 16.02.2023

Revised 16.02.2023

Accepted 04.04.2023

М. М. Сальніков, голов. наук. співроб., д-р фіз.-мат. наук

ORCID <https://orcid.org/0000-0001-9810-0963>

E-mail: salnikov.nikolai@gmail.com.

С. В. Мельничук, старш. наук. співроб., канд. техн. наук

ORCID <https://orcid.org/0000-0002-6027-7613>

E-mail: sergvik@ukr.net.

В. Ф. Губарев, зав. відділу, чл.-кор. НАН України, професор, д-р техн. наук

ORCID <https://orcid.org/0000-0001-6284-1866>

E-mail: v.f.gubarev@gmail.com.

Л. В. Максимюк, наук. співроб., канд. техн. наук

ORCID <https://orcid.org/0000-0002-2561-109X>

E-mail: hatahatky@gmail.com.

В. М. Шевченко, старш. наук. співроб., канд. фіз.-мат. наук

ORCID <https://orcid.org/0000-0002-1304-9124>

E-mail: vovan_16@ukr.net.

Інститут космічних досліджень Національної академії наук України та Державного космічного агентства України
пр. Академіка Глушкова 40, корп. 4/1, Київ 187, Україна, 03187

ОЦІНЮВАННЯ ПАРАМЕТРІВ ВІДНОСНОГО РУХУ НЕКООПЕРОВАНОГО КОСМІЧНОГО АПАРАТА ЗА ВІЗУАЛЬНОЮ ІНФОРМАЦІЄЮ

Розглянуто задачу визначення параметрів відносного руху некооперованого космічного апарата (НКА), що перебуває у вільному некерованому русі, за результатами вимірювання відстані до цього апарата та його кватерніона орієнтації. Припускається, що ці вимірювання виконуються системою технічного зору (СТЗ). Конкретний тип СТЗ не розглядається. Припускається, що СТЗ вимірює відстань та положення так званої графічної системи координат, яка жорстко закріплена на НКА. До параметрів відносного руху належать вектор відстані до центра мас НКА, кватерніон орієнтації головних осей інерції НКА відносно системи координат СТЗ, кватерніон орієнтації графічної системи координат відносно головної системи координат НКА, відношення моментів інерції, вектор положення центра мас у графічній системі координат. Задача вирішується за допомогою динамічного фільтра, оснований на методі еліпсоїдального оцінювання. Метод передбачає знання лише максимальних значень шуму вимірів, стохастичні характеристики шуму не передбачаються відомими і тому не використовуються. Властивості запропонованого алгоритму було продемонстровано за допомогою чисельного моделювання. Отримані результати планується використовувати для розробки, створення та випробування навігаційної системи зближення та стикування сервісного космічного апарата, що розробляється групою підприємств космічної галузі України під керівництвом ТОВ «Курс-Орбітал».

Ключові слова: параметри відносного руху, космічний апарат, оцінювання, відео.